



This is a repository copy of *Preventing phosphorylation of dystroglycan ameliorates the dystrophic phenotype in mdx mouse*.

White Rose Research Online URL for this paper:
<http://eprints.whiterose.ac.uk/129500/>

Version: Accepted Version

Article:

Miller, G. orcid.org/0000-0003-4527-3814, Moore, C.J., Terry, R. et al. (6 more authors) (2012) Preventing phosphorylation of dystroglycan ameliorates the dystrophic phenotype in mdx mouse. *Human Molecular Genetics*, 21 (20). pp. 4508-4520. ISSN 0964-6906

<https://doi.org/10.1093/hmg/dds293>

Reuse

Unless indicated otherwise, fulltext items are protected by copyright with all rights reserved. The copyright exception in section 29 of the Copyright, Designs and Patents Act 1988 allows the making of a single copy solely for the purpose of non-commercial research or private study within the limits of fair dealing. The publisher or other rights-holder may allow further reproduction and re-use of this version - refer to the White Rose Research Online record for this item. Where records identify the publisher as the copyright holder, users can verify any specific terms of use on the publisher's website.

Takedown

If you consider content in White Rose Research Online to be in breach of UK law, please notify us by emailing eprints@whiterose.ac.uk including the URL of the record and the reason for the withdrawal request.



eprints@whiterose.ac.uk
<https://eprints.whiterose.ac.uk/>

Published in final edited form as:

Hum Mol Genet. 2012 October 15; 21(20): 4508–4520. doi:10.1093/hmg/dds293.

Preventing phosphorylation of dystroglycan ameliorates the dystrophic phenotype in *mdx* mouse

Gaynor Miller¹, Chris J. Moore², Rebecca Terry³, Tracy La Riviere², Andrew Mitchell², Robert Piggott², T. Neil Dear^{1,4}, Dominic J. Wells³, and Steve J. Winder^{2,*}

¹Department of Cardiovascular Science, University of Sheffield, Firth Court, Western Bank, Sheffield, S10 2TN, UK

²Department of Biomedical Science, University of Sheffield, Firth Court, Western Bank, Sheffield, S10 2TN, UK

³Department of Veterinary Basic Science, Royal Veterinary College, Royal College Street, London NW1 0TU, UK

Abstract

Loss of dystrophin protein due to mutations in the DMD gene causes Duchenne muscular dystrophy. Dystrophin loss also leads to the loss of the dystrophin glycoprotein complex (DGC) from the sarcolemma which contributes to the dystrophic phenotype. Tyrosine phosphorylation of dystroglycan has been identified as a possible signal to promote the proteasomal degradation of the DGC. In order to test the role of tyrosine phosphorylation of dystroglycan in the aetiology of DMD we generated a knock-in mouse with a phenylalanine substitution at a key tyrosine phosphorylation site in dystroglycan – Y890. Dystroglycan knock-in mice (*Dag1*^{Y890F/Y890F}) had no overt phenotype. In order to examine the consequence of blocking dystroglycan phosphorylation on the aetiology of dystrophin-deficient muscular dystrophy, the Y890F mice were crossed with *mdx* mice an established model of muscular dystrophy. *Dag1*^{Y890F/Y890F}/*mdx* mice showed significant improvement in several parameters of muscle pathophysiology associated with muscular dystrophy including; reduction in centrally nucleated fibres, less Evans blue dye infiltration and lower serum creatine kinase levels. With the exception of dystrophin, other DGC components were restored to the sarcolemma including α -sarcoglycan, α - β -dystroglycan and sarcospan. Furthermore, *Dag1*^{Y890F/Y890F}/*mdx* showed a significant resistance to muscle damage and force loss following repeated eccentric contractions when compared to *mdx* mice. Whilst the Y890F substitution may prevent dystroglycan from proteasomal degradation an increase in sarcolemmal plectin appeared to confer protection on *Dag1*^{Y890F/Y890F}/*mdx* mouse muscle. This new model confirms dystroglycan phosphorylation as an important pathway in the aetiology of DMD and provides novel targets for therapeutic intervention.

*Corresponding author s.winder@sheffield.ac.uk, Tel 0114 222 2332.

⁴Current address: Leeds Institute of Molecular Medicine, Wellcome Trust Brenner Building, St. James's University Hospital, Leeds, UK

The authors wish it to be known that, in their opinion, the first 2 authors should be regarded as joint First Authors.

Introduction

In normal striated muscle dystrophin associates with a large group of proteins known as the dystrophin glycoprotein complex (DGC) (1). The DGC serves to stabilise the sarcolemma by making regularly spaced connections between the muscle fibre cytoskeleton and extracellular matrix – part of the costameric cell adhesion complex (2). At the core of this cell adhesion complex is the adhesion receptor dystroglycan, which binds laminin in the extracellular matrix and dystrophin on the cytoplasmic face (3). Like many cell adhesion complexes, the DGC also has associated signalling activity, in particular we have indentified tyrosine phosphorylation of dystroglycan as an important regulatory event in controlling the integrity of the DGC (4). Previous studies from the Lisanti group and ourselves suggested that tyrosine phosphorylation of dystroglycan is an important mechanism for controlling the association of dystroglycan with its cellular binding partners dystrophin and utrophin, and also as a signal for degradation of dystroglycan (5–7). The Lisanti group further demonstrated that inhibition of the proteasome was able to restore other DGC components in both *mdx* mice that lack dystrophin and in explants of DMD patients (8, 9). From these studies it can be concluded that under normal circumstances binding of dystrophin to dystroglycan via the WW domain binding motif PPPY890 prevents tyrosine phosphorylation of β -dystroglycan thus allowing the DGC to be maintained stably at the sarcolemma. However, with dystrophin deficiency i.e. in DMD patients or in the *mdx* mouse, the WW domain binding motif in dystroglycan is exposed allowing Y890 to become phosphorylated which targets dystroglycan for degradation and results in the loss of the entire DGC from the sarcolemma.

Previously, it has been demonstrated that restoration of the DGC by Dp71 overexpression did not alleviate the dystrophic phenotype in *mdx* mice (10, 11). We surmise that this approach fails because whilst the dystrophin and utrophin binding site on dystroglycan is blocked by Dp71 and the complex is restored, Dp71 cannot bind to the actin cytoskeleton, so the link between extracellular matrix and cytoskeleton remains compromised. Furthermore, simple transgenic overexpression of dystroglycan in *mdx* is also not able to ameliorate the muscular dystrophy phenotype (12), probably because it is still susceptible to phosphorylation and subsequent degradation. We have therefore investigated whether preventing dystroglycan phosphorylation in mouse by a targeted gene knock-in of phenylalanine at tyrosine residue 890, which is predicted to block tyrosine phosphorylation, can restore dystroglycan function and reduce the dystrophic phenotype in *mdx* mice.

Results

Generation of a *Dag1*^{Y890F} mouse

In order to assess the role of Y890 in regulating dystroglycan function *in vivo*, a targeted substitution of tyrosine 890 to phenylalanine (Y890F) was generated in mouse using standard techniques: homologous recombination in ES cells (see Figure 1), injection into blastocyst, selection of germline transmission of the targeting construct. Both heterozygous and homozygous *Dag1*^{Y890F} mice appeared normal and healthy and were born at expected Mendelian ratios. To date in mice up to 8 months old, no deleterious effect of the substitution has been noted. Western blot and immunohistochemistry analysis of

heterozygous and homozygous *Dag1*^{Y890F} revealed normal levels of total β -dystroglycan compared to wildtype, but with reduced levels of detectable pY890 β -dystroglycan in heterozygotes and an absence in homozygotes (Figure 1F-I).

Preventing dystroglycan phosphorylation on tyrosine 890 reduces muscle pathology in dystrophic mice

—In order to assess whether the introduction of a Y890F substitution in dystroglycan had any beneficial effect on dystrophin deficiency, *Dag1*^{Y890F/Y890F}/*mdx* mice were generated. Samples of muscle and serum from wildtype, *Dag1*^{Y890F/Y890F}, *mdx* and *Dag1*^{Y890F/Y890F}/*mdx* mice were examined for markers of muscle damage including serum creatine kinase levels and centrally nucleated fibres. The introduction of the Y890F substitution into dystroglycan by itself had no effect on pathophysiological parameters of muscle and compared to wildtype, haematoxylin and eosin stained sections of *Dag1*^{Y890F/Y890F} muscle appeared normal (Figure 2A,B). However, when crossed with *mdx*, *Dag1*^{Y890F/Y890F} caused a significant reduction in the numbers of centrally nucleated fibres (Figure 2C-E) and the levels of serum creatine kinase (Figure 2F). The number of fibres with centrally located nuclei was decreased by 35% and the levels of serum creatine kinase were halved when compared to *mdx* alone. The improvement in muscle pathophysiology in *Dag1*^{Y890F/Y890F}/*mdx* compared to *mdx* is consistent with an overall reduction in muscle damage as indicated by the reduced leakage of creatine kinase into the blood stream from *Dag1*^{Y890F/Y890F}/*mdx* muscle. Moreover, the reduction in central fibre nucleation likely reflects a reduction in muscle regeneration as a consequence of reduced degeneration. Therefore at the level of histopathology the Y890F substitution in dystroglycan appears to have significantly reduced the dystrophic phenotype observed in *mdx* mice.

Preventing dystroglycan phosphorylation on tyrosine 890 restores sarcolemmal expression of the DGC in dystrophic mice

—The absence of dystrophin in muscle leads to a significant reduction in the other components of the DGC from the sarcolemma (13). This in turn leads to a perturbation in the connection between the extracellular matrix and intracellular actin cytoskeleton which is thought to be one of the main reasons for the contraction induced muscle damage observed with dystrophin deficiency (14). Preventing phosphorylation of dystroglycan on tyrosine 890 had no obvious detrimental effects on the localisation of the following key members of the DGC: α - and β -dystroglycan, dystrophin, α -sarcoglycan and sarcospan (Figure 3) or on the localisation of laminin in the extracellular matrix and utrophin in the neuromuscular junction. However, preventing phosphorylation of dystroglycan in the absence of dystrophin i.e. in *Dag1*^{Y890F/Y890F}/*mdx* muscle restored α - and β -dystroglycan, α -sarcoglycan and sarcospan to the sarcolemma (Figure 3). Laminin was maintained in the sarcolemma of *Dag1*^{Y890F/Y890F}/*mdx* muscle at similar levels to those found in wild-type and *mdx* muscle (Figure 3). In previous studies sarcolemmal utrophin was shown to be upregulated in DMD and *mdx* muscle (15, 16). In the *Dag1*^{Y890F/Y890F}/*mdx* muscle sarcolemma however, utrophin staining returned to the more restricted neuromuscular junction distribution seen in wild-type muscle (Figure 3 and Supplementary Figure 1). Therefore, in the absence of dystrophin the Y890F substituted dystroglycan was not only protected from degradation but also contributed to the preservation of the normal distribution of other DGC components.

Interestingly the Y890F substituted dystroglycan did not support the extrasynaptic localisation of utrophin seen in *mdx* alone (Supplementary Figure 1), but this could be due to the utrophin WW domain not binding efficiently to the phenylalanine substituted WW domain binding motif (6). The staining of muscle sections with laminin gave the impression that there was an increase in the number of smaller muscle fibres in the *Dag1^{Y890F/Y890F}* mice. Quantification of fibre size did reveal an approximate 25% reduction in mean minimum Ferret's diameter in *Dag1^{Y890F/Y890F}* mice but this was not significant, nor was it associated with any apparent change in fibre type based on assessment of glycolytic activity nor any change in specific force (Supplementary Figures 2-4). Measurement of muscle weight and size from age matched mice also revealed a slight but non-significant reduction in calculated muscle cross-sectional area (data not shown). Moreover, fibre number counts of whole quadriceps sections did not reveal any significant difference between mouse genotypes (Supplementary Figure 2).

Although from the immunofluorescence analysis there are clear changes in both the apparent amounts and localisation of DGC components (Figure 3). Quantification of actual protein levels by western blotting suggest that most of the changes observed by immunofluorescence are due to either loss of protein by degradation (in the case of *mdx*) or redistribution of protein within the muscle fibre rather than any actual increase in protein synthesis in the case of *Dag1^{Y890F/Y890F}/mdx* (Figure 4). As expected from their respective genotypes, Dp427 dystrophin was absent from *mdx* and *Dag1^{Y890F/Y890F}/mdx* mice, and pY890 β -dystroglycan was not detectable in *Dag1^{Y890F/Y890F}* or *Dag1^{Y890F/Y890F}/mdx* mice. Whilst there was an apparent change in unphosphorylated β -dystroglycan levels in the different mice this was to be expected as both of the antibodies most commonly used to detect β -dystroglycan (43DAG/8D5 and MANDAG2) have Y890 in their epitope ((6) and Supplementary Figure 5) so are sensitive to the Y890F substitution. Attempts to generate antisera against a Y890F substituted peptide were not successful. Moreover it is well documented that β -dystroglycan levels are reduced in *mdx* though not absent (see (17) for example). As expected, utrophin levels appear increased in *mdx* mice, however western blot analysis suggests an increase in *Dag1^{Y890F/Y890F}* and *Dag1^{Y890F/Y890F}/mdx* mice too (Figure 4A). Utrophin is apparent at NMJ in all mice (Figure 3 and Supplementary Figure 1), but despite the apparent upward trend in total utrophin levels in *Dag1^{Y890F/Y890F}*, *mdx* and *Dag1^{Y890F/Y890F}/mdx* (Figure 4C), a redistribution of utrophin to the sarcolemma is only apparent in *mdx* (Figure 3 and Supplementary Figure 1).

***In vitro* analysis of pY890 β -dystroglycan**

Western blotting of mouse muscle with an antibody against pY890 β -dystroglycan (antibody 1709 (5)) revealed as expected a complete absence of β -DG phosphorylation on tyrosine 890 in muscle samples (Figure 4), this not only verified the genetic change at the protein level, but provided further evidence for the specificity of our pY890 antiserum 1709 (see also Supplementary Figure 5). However to further confirm the fate of phosphorylated β -DG in muscle cells we carried out surface biotinylation experiments to determine the role of β -dystroglycan phosphorylation in the internalisation process. Previous analysis of dystroglycan function by microscopy in Cos-7 cells has revealed a phosphorylation-dependent internalisation of β -dystroglycan in response to constitutive Src activation (7). In

order to more rigorously determine the role of dystroglycan phosphorylation on tyrosine 890 in this process, we analysed the fate of dystroglycan in normal immortalised H2k myoblast cells (18) over time using a cell surface biotinylation assay. We monitored non-phosphorylated β -dystroglycan with the monoclonal antibody MANDAG2 (19) which is sensitive to the phosphorylation of β -dystroglycan at Y890 (6), and monitored β -dystroglycan phosphorylated at Y890 with antibody 1709 (5) which is specific for Y890 phosphorylated dystroglycan and does not detect unphosphorylated β -dystroglycan (Supplementary Figure 5). Following cell-surface biotinylation, in contrast to non-phosphorylated β -dystroglycan which was detected on the membrane only and not in the internalised fraction, tyrosine phosphorylated β -dystroglycan was detected at the cell surface and in the cytosol (Figure 5A). Furthermore, there was a time-dependent decrease in the amount of cell surface phosphorylated β -dystroglycan and a concomitant increase in cytosolic phosphorylated β -dystroglycan (Figure 5A). These data suggest therefore that phosphorylation of β -dystroglycan on tyrosine 890 is a signal for the internalisation and potentially the degradation of β -dystroglycan. In support of this, immunofluorescence localisation of intracellular vesicles containing β -dystroglycan with either MANDAG2 or 1709 antibodies revealed differing cellular distributions with respect to each other and to transferrin receptor containing endocytic vesicles (Supplementary Figure 6). These findings demonstrate that in normal myoblasts phosphorylated dystroglycan is found in larger vesicles consistent with its internalisation upon phosphorylation. These larger vesicles do not colocalise with early endosomal antigen 1 (EEA1) nor with lysotracker and these vesicles are distinct from transferrin containing vesicles (Supplementary Figure 6). This suggests that internalisation of phosphorylated dystroglycan occurs via an endocytic process that is independent of clathrin and is potentially trafficked via a novel route/compartments.

Preventing dystroglycan phosphorylation on tyrosine 890 confers partial protection against contraction induced injury in dystrophic mice

—Given the marked improvement in histopathology and the clear restoration of DGC components in *mdx* mice expressing Y890F dystroglycan, we examined the extent of any functional improvement in mouse muscle. To assess the functional benefit of preventing dystroglycan phosphorylation on tyrosine 890, TA muscles from anaesthetised *Dag1*^{Y890F/Y890F}/*mdx* were subjected to a protocol of 10 eccentric (lengthening) contractions *in situ*. The protocol induced a 10% stretch during each of 10 maximal isometric contractions stimulated 2 minutes apart. Isometric tetanic force was measured prior to each stretch and expressed as a percentage of baseline isometric force.

Gene targeted *Dag1*^{Y890F/Y890F} mice did not demonstrate a drop in isometric force during the eccentric contraction protocol (data not shown) which is similar to wild-type mice (20). When *Dag1*^{Y890F/Y890F} mice were crossed with *mdx* mice a modest but highly significant improvement in resistance to eccentric contraction-induced injury was seen compared to *mdx* control mice of the same age ($P=0.006$; Figure 6). Specifically *Dag1*^{Y890F/Y890F}/*mdx* mice were significantly stronger than control mice after eccentric contractions 5, 6 and 7 ($P=0.025$, 0.025 and 0.040 respectively; Figure 6). Maximum isometric specific force produced by *Dag1*^{Y890F/Y890F}/*mdx* mice was 13.5 ± 0.745 N/cm² which was not significantly different from *mdx* control mice. There was also no significant difference in the force-

frequency curves between *Dag1*^{Y890F/Y890F}/*mdx* and *mdx* mice (Supplementary Figure 4) or TA muscle size (Supplementary Table 1).

The physiological studies described above demonstrate that the Y890F substitution not only reduces muscle damage and restores DGC components at the sarcolemma, but can also contribute to a modest but significant improvement in resistance to eccentric contraction in *mdx* muscle.

Preventing dystroglycan phosphorylation on tyrosine 890 increases levels of plectin in the sarcolemma of dystrophic mice—Given the role of dystroglycan as an adhesion receptor and scaffold for several cytoskeletal anchoring proteins (4) we might hypothesise that the most likely candidate to contribute to the dystroglycan Y890F mediated rescue of the *mdx* phenotype would be utrophin. As discussed above utrophin is naturally upregulated in DMD and *mdx* muscle (15, 16), is known to bind to dystroglycan (6), and is itself protective when overexpressed in *mdx* muscle (21). However utrophin was not localised to the sarcolemma in *Dag1*^{Y890F/Y890F}/*mdx* muscle (Figure 3 and Supplementary Figure 1). Therefore, improvement in the dystrophic phenotype i.e. decreased number of centrally located nuclei, reduction in serum creatine kinase levels and the improvement in resistance to eccentric contraction-induced injury, which was observed by preventing dystroglycan phosphorylation on tyrosine 890 cannot be attributed to an increase in sarcolemmal utrophin. Plectin is a cytolinker protein predominantly found in skeletal muscle where it is localised at the sarcolemma, z-disks and mitochondria. Plectin is also upregulated in dystrophin deficient muscle (22). Plectin interacts with β -dystroglycan at multiple sites in the cytoplasmic domain (22), therefore its interaction may not be affected directly by phosphorylation of β -dystroglycan or by the substitution of Y890 to phenylalanine. We therefore investigated whether plectin could be providing the link between dystroglycan and the actin cytoskeleton in the absence of dystrophin in the *Dag1*^{Y890F/Y890F}/*mdx* muscle. Samples of wild-type, *Dag1*^{Y890F/Y890F}, *mdx* and *Dag1*^{Y890F/Y890F}/*mdx* muscle were examined for expression and localisation of plectin (Figure 7). Consistent with our previous findings (22), plectin immunolocalisation at the sarcolemma is low in wildtype muscle but increased in *mdx* muscle where it appears to preferentially stain regenerating fibres i.e. those with centrally located nuclei. Surprisingly however, in *Dag1*^{Y890F/Y890F} muscle, plectin staining of the sarcolemma appeared to be increased uniformly when compared to wildtype muscle (Figure 7A,B). Furthermore, the increase in plectin staining was also observed at the sarcolemma of *Dag1*^{Y890F/Y890F}/*mdx* muscles when compared to *mdx* muscle (Figure 7C,D). However total plectin levels revealed by western blotting (Figure 7E) may not accurately reflect specific changes in individual isoforms, as it is known that plectin 1f is the predominant isoform localised at the costameres at the sarcolemma (22), whereas plectin isoforms 1, 1d and 1b are associated with nuclei, Z discs and mitochondria respectively (23). Our findings support the hypothesis that phosphorylation of dystroglycan on Y890 is a key event in the aetiology of the dystrophic phenotype in the *mdx* mouse and that plectin is a candidate to maintain the link between the extracellular matrix and the cytoskeleton in the absence of dystrophin.

Discussion

This study demonstrates that preventing phosphorylation of a key tyrosine residue on murine dystroglycan -Y890, ameliorates many of the main pathological symptoms associated with dystrophin deficiency in the *mdx* mouse. Muscle degeneration/regeneration was reduced as shown by a decrease in the number of centrally located nuclei, myofibre integrity was increased with a 50% reduction in serum creatine kinase levels, whilst there was also restoration of DGC components to the sarcolemma and an improvement in the resistance to eccentric contraction-induced injury. The Y890F mutation alone did not appear to have any detrimental side effects, with the only observed change from wildtype being a slight reduction in fibre diameter and an increase in plectin staining at the sarcolemma. The overt health of the Y890F knock-in mice, and the significant improvement in dystrophic pathology observed when crossed onto an *mdx* background, identifies dystroglycan phosphorylation as a potential therapeutic target and provides a new paradigm for the treatment of DMD. Although in this study we have used a genetic approach to remove an important phosphorylation site in dystroglycan, future therapeutic approaches would be aimed at targeting the signalling pathways that lead to the phosphorylation of dystroglycan or the subsequent degradation process.

The potential for therapeutic restoration of dystroglycan function to the sarcolemma has been assessed previously, but without success. Restoration of dystrophin or utrophin in *mdx* mice, by genetic, viral or chemical means is able to restore dystroglycan and other DGC components and effect a significant rescue of the dystrophic phenotype, indeed a number of therapeutic strategies are predicated on the success of this approach. In these cases however, a 'corrected' dystrophin (exon skipping strategies), a replacement dystrophin (gene and cell based approaches) or a dystrophin homologue (utrophin upregulation) is required to achieve a functional rescue, see (24, 25) for recent reviews. In all these cases there was an attempt to restore a fully functional DGC with appropriate connections between extracellular matrix and sarcolemmal cytoskeleton. Other approaches have attempted to restore the DGC by different means, including transgenic overexpression of Dp71 a short 3' product of the *Dmd* gene that includes the WW domain that provides interactions with dystroglycan (10, 11), or by simply overexpressing dystroglycan in order to increase the amount at the sarcolemma (12). High level overexpression of Dp71 in *mdx* increases DGC components at the sarcolemma but does not result in the redistribution/downregulation of utrophin, nor does it improve other aspects of the dystrophic pathology (10, 11). At first sight these data appear paradoxical, but if one considers that the level of utrophin upregulation present is no different from *mdx*, which in itself cannot be fully protective as there is a dystrophic phenotype. Utrophin clearly does exert some protective function, as knockout of utrophin in *mdx* leads to a much more severe phenotype (26, 27). However, even in the presence of some utrophin and with an increase in other DGC components Dp71 cannot make connections to the cytoskeleton and therefore does not stabilise the sarcolemma (10, 11). As the authors of both these studies discuss, restoration of the DGC is by Dp71 binding to dystroglycan and reduction of DGC component degradation. From our studies we would further surmise that this is due to the protective effect of Dp71 binding to β -dystroglycan via the PPPY motif and reducing tyrosine phosphorylation and as a consequence dystroglycan

degradation. By similar reasoning, we hypothesise that simply overexpressing dystroglycan also fails to rescue the dystrophic *mdx* phenotype in the same manner. Whilst elevated levels of both α - and β -dystroglycan and a significant increase in sarcolemmal localisation of these proteins have been achieved in muscle by transgenic overexpression, there was not a concomitant increase in utrophin or sarcoglycan, nor was there any improvement in dystrophic pathology (12). In this case there may be three factors which taken together explain the failure of increased dystroglycan to rescue the dystrophic phenotype: first is that even though dystroglycan levels are increased, possibly because there is not a coordinated upregulation of sarcoglycans and other DGC proteins, the complexes formed at the sarcolemma are not competent to stabilise the sarcolemma. Secondly, as in the case of Dp71 overexpression, there is no increase in a cytolinker protein such as utrophin that can provide the link to the extracellular matrix and thirdly, whilst dystroglycan levels are increased, dystroglycan may be turned over rapidly as it could be susceptible to phosphorylation mediated degradation. In the present study by contrast, dystroglycan is expressed at normal levels from its own promoter, tyrosine 890 has been substituted to phenylalanine so cannot be phosphorylated. Although utrophin levels do not remain elevated, plectin expression/localisation at the sarcolemma is increased providing a stabilising link from dystroglycan to the cytoskeleton. The data presented here describing the rescue of the dystrophic phenotype achieved in *mdx* by changing a single phosphorylation site in dystroglycan, represents a new paradigm in the aetiology and potential treatment of DMD.

We hypothesised that phosphorylation of dystroglycan targets it for degradation. Previous work from the Lisanti group had identified Src, but not other Src family kinases or FAK, as capable of phosphorylating dystroglycan on Y890 (28), and that pY890 dystroglycan was internalised into vesicular structures that colocalised with cSrc when dystroglycan and cSrc were co-expressed in Cos-7 cells (7). Furthermore immunofluorescence localisation of pY890 β -dystroglycan in normal mouse muscle revealed a punctate staining pattern in the interior of the fibres and not at the sarcolemma as seen with non-phosphorylated dystroglycan (7). Using a membrane targeted β -dystroglycan cytoplasmic domain construct, they also demonstrated that the β -dystroglycan construct was targeted to late endosomes dependent on Src phosphorylation of Y890 (7). These data are consistent with our own findings in myoblast cells (figure 5) that only endogenous phosphorylated β -dystroglycan is internalised from the membrane. The fate of internalised phosphorylated β -dystroglycan, it has not been demonstrated whether α -dystroglycan is also internalised, is presumed to be proteasomal degradation – along with other DGC components that are internalised in *mdx* and DMD. Based on this premise, it has been proposed that blocking the ultimate step in the pathway, namely the proteasome, might be able to restore DGC components to the sarcolemma (8). Treatment with proteasomal inhibitors does indeed restore dystroglycan and other DGC components to the membrane and in appropriate models can be demonstrated to improve muscle pathophysiology in: *mdx* mice, explants from DMD and BMD patients and in *sapje* a zebrafish model of DMD (8, 9, 29–31). Our mouse genetic model also suggests that blocking the first step in the pathway – namely tyrosine phosphorylation of β -dystroglycan also has specific and beneficial effects in improving the dystrophic phenotype. Consequently appropriate therapeutic agents that inhibit Src kinase may also prove to be beneficial in treating DMD. Like proteasomal inhibitors however, clinically approved

tyrosine kinase inhibitors, mostly in use as anti-cancer agents, have significant side effects. However, having identified drugable targets at two different points in a pathway leading to the loss of dystroglycan and DGC function in DMD, it should be possible to apply combinatorial therapies to achieve synergistic effects at much lower doses thus alleviating the side effects.

Utrophin upregulation occurs spontaneously to a certain extent in DMD (32, 33) and also in *mdx* (15, 16) where it has a clear protective effect (26, 27). Furthermore, forced expression of utrophin ameliorates the dystrophic phenotype in *mdx*, whether via a transgene (21), or by enhancing promoter activity pharmacologically (34). Moreover, as noted above, Dp71 overexpression in *mdx* protects the DGC and maintains levels of utrophin seen in *mdx* alone. By stabilising dystroglycan and other DGC components at the sarcolemma we therefore expected to achieve a rescue of the dystrophic phenotype in part by the actions of utrophin in anchoring the DGC to the sarcolemma. As our data show however, utrophin levels were not maintained in *mdx* expressing Y890F dystroglycan, but instead, plectin levels were upregulated. This unexpected finding raises some interesting questions: when the DGC is restored by preventing dystroglycan phosphorylation what are the mechanisms that lead to the preferential increase in plectin rather than utrophin at the sarcolemma, and how can plectin apparently effect such a rescue of the *mdx* phenotype? From the phenotypes of epidermolysis bullosa simplex with muscular dystrophy, we know that mutations in plectin contribute to sarcolemmal integrity (35–37), and that plectin is enriched at the sarcolemma in DMD (38) and plectin 1f specifically in the costameres of *mdx* mice (22). More recently a mutation in exon 1f of plectin has been shown to give rise to an autosomal recessive limb girdle muscular dystrophy (LGMD2) phenotype independently of any dermatological symptoms (39). Therefore plectin, like utrophin, is one of the family of large cytolinker proteins that contribute to sarcolemmal integrity and are naturally upregulated, or redistributed, in a protective role in dystrophic muscle. From this brief review of plectin function in muscle, it is clear that plectin is already contributing to muscle architecture and is naturally upregulated in dystrophic conditions. But why plectin and not utrophin localisation to the sarcolemma in our Y890F/*mdx* model? Part of the answer may lie in the nature of the mutation that was introduced into dystroglycan in this study. Changing the WW domain interaction motif PPPY to PPPF would not be predicted to support efficient binding of the utrophin WW domain (6, 40, 41). Our previous biochemical analysis of plectin, dystrophin and dystroglycan interactions (22), reveals the ability of plectin to bind to two sites on dystroglycan, including one that overlaps with the dystrophin WW domain interaction site – but importantly is not itself a WW domain interaction as plectin does not contain a WW domain. As previously published, in the *mdx* mouse, plectin can bind to dystroglycan through both interaction sites including the c-terminal PPPY motif (22). Plectin upregulation is likely to be more effective at rescuing the dystrophic phenotype in *mdx*/Dag1^{Y890F/Y890F} because dystroglycan is protected from degradation, whereas in *mdx* it is not, and plectin is unable to stabilise the sarcolemma. In the Y890F mouse the ability of dystrophin to interact with the mutated PPPF motif is also weakened allowing increased plectin binding. In the *mdx*/Y890F mouse where dystroglycan phosphorylation is prevented and is therefore stabilised at the sarcolemma, plectin interaction/recruitment at the sarcolemma is further enhanced leading to a partial rescue of the dystrophic phenotype. The

scheme put forward in our 2007 publication (see figure 10 in (22)) to explain the role of plectin in *mdx* mouse, also fits well with the role of plectin in our *mdx/Y890F* mouse model. We cannot rule out a role for increased utrophin levels in the rescue of the *mdx* phenotype, however it is unlikely that these alone are sufficient. It is possible that interactions between plectin and utrophin could replace interactions between plectin and dystrophin, but this is not supported by available utrophin localisation data in the *Dag1^{Y890F/Y890F}* or *Dag1^{Y890F/Y890F}/*mdx** muscle. More detailed examination of the interactions between plectin, dystroglycan and utrophin are clearly warranted.

Thus we have developed a new model of muscular dystrophy that for the first time not only reveals the importance of dystroglycan phosphorylation in the aetiology of muscular dystrophy, but also provides a new rationale for therapeutic intervention in Duchenne muscular dystrophy. Whether combinatorial drug treatment using both proteasomal and tyrosine kinase inhibitors would provide sufficient therapeutic benefit on its own remains to be tested, however the promising genetic (this study) and pharmacological (8, 9, 29–31) interventions suggest at the very least that these approaches could be powerful adjuncts to other therapies such as exon skipping or utrophin upregulation.

Materials and Methods

Generation of a *Dag1^{Y890F}* targeting construct

To generate the targeting vector a 9.8kb *XhoI-EcoRI* fragment that included a portion of intron 1 and the entire exon 2 of the *Dag1* gene was subcloned from bacterial artificial chromosome (BAC) clone bmQ433-E3 (GeneService) into similarly digested pBluescript SK(+)vector. The A to T nucleotide change (underlined) corresponding to the Y890F substitution was introduced by site directed PCR mutagenesis using the forward primer (5' - ATACCGATCACCCCCTCCGTTTGTTC^{CCCCCT}-3') and reverse primer (5' - ACGGAGGGGGTGATCGGTATGGGGTCATGT-3') and the GeneTailor™ site-directed mutagenesis System (Invitrogen). A *BclI* site in intron 1 was used to insert the phosphoglycerate Kinase (PGK) neomycin resistance selection cassette flanked by lox P sites. In addition *HpaI* and *XhoI* sites in the vector backbone, outside the region of homology, were used to insert a PGK DTA cassette for negative selection. The final targeting vector (see figure 1A) was verified by restriction digest and direct sequencing.

After linearization of the targeting vector using *XhoI*, embryonic stem (ES) cell electroporation and blastocyst injection was performed by the Mouse Engineering Services of the University of Sheffield (MESUS).

Verification of the correct recombination event within neomycin resistant protamine-Cre (42) ES cell clones was performed by Southern analysis of *EcoRI* and *KpnI* digested genomic DNA using a probe located within intron 1 (Fig. 1A). WT chromosomes resulted in a 16.4 kb *EcoRI* fragment and a 6.8kb *KpnI* fragment (Fig. 1A and 1B). Properly targeted chromosomes produced a smaller 5.8 kb *EcoRI* fragment resulting from the presence of an additional *EcoRI* site within the neomycin resistance cassette and a larger 8.6kb *KpnI* fragment resulting from the insertion of the ~1.8 kb neomycin cassette (Fig. 1A and 1B). Genomic DNA from positive clones and subsequent progeny was also amplified and

sequenced to confirm the presence of the point mutation (Fig 1C). In male chimeras, when PC3 ES cells differentiate into spermatids, Cre recombinase is expressed and results in the excision of the floxed PGK- Neo cassette (42). Excision of the Neo cassette was confirmed in this chimera and subsequent progeny by PCR using one set of primers that flank the loxP sites as follows: forward primer 5' -ATGAGTTGGATTTCCCAGCA-3' and reverse primer 5' -ATGGCCTGGCCTAAAATGAT-3' giving rise to the following products: 104bp in WT progeny(+); 177bp in progeny with the neo cassette excised (Neo-) but retaining a single loxP site and 1872 bp (not shown) in progeny where the neo cassette is still intact (Neo+, Fig 1D) and another that utilise the same forward primer and a reverse primer located in the neo gene 5' -ATCGCCTTCTATCGCCTTCT-3' giving rise to a 499bp product where the neo cassette is still intact and no product in WT and neo excised progeny (Fig. 1D).

Chimaeric animals were then bred to heterozygosity by crossing with C57Bl6 mice. Sequencing of the *Dag1* gene in targeted heterozygotes demonstrated equal proportions of both the WT adenine and MUT thymidine bases specifying the p.Y890F substitution (Fig. 1C). Breeding to homozygous WT or MUT genotypes was confirmed by PCR amplification, restriction enzyme digestion and agarose gel electrophoresis (Fig. 1E, see Genotyping section below). Homozygous WT, heterozygous *Dag1*^{Y890F/+} and homozygous *Dag1*^{Y890F/Y890F} (MUT) mice at the specified ages were used in subsequent studies. To examine the effect of the Y890F mutation on muscle pathology in dystrophin deficient muscular dystrophy *Dag1*^{Y890F/Y890F} mice were backcrossed with *Dmd*^{mdx/mdx} mice (Generous gift from Steve Laval, Newcastle) for 4 generations. Mice heterozygous for the Y890F mutation and either homozygous or hemizygous for the mdx mutation (*Dag1*^{Y890F/+}/*Dmd*^{mdx/Y} or *Dag1*^{Y890F/+}/*Dmd*^{mdx/mdx}) were crossed to generate double homozygous offspring of both sexes (*Dag1*^{Y890F/Y890F}/*Dmd*^{mdx/Y} and *Dag1*^{Y890F/Y890F}/*Dmd*^{mdx/mdx}) and male mice that were hemizygous for the mdx mutation and heterozygous for the Y890F *Dag1* mutation (*Dag1*^{Y890F/+}/*Dmd*^{mdx/Y}) for use in our subsequent studies.

All animals were maintained in a high health status facility at the University of Sheffield according to the UK Home Office guidelines with access to food and water *ad libidum*. All animal studies were approved by both the ethical committee at the University of Sheffield and the UK Home Office.

Genotyping—Mouse ear biopsies were lysed overnight at 55°C in tail lysis buffer (50mM TrisHCl pH 8.5; 2mM EDTA pH 8; 0.5% Tween; 300mg/ml Proteinase K) and used for genotyping by PCR. Genotyping for *Dag1*^{Y890F/Y890F} mutants was performed by PCR amplification of a 107 bp fragment of the *Dag1* gene using the forward primer 5' -ATACCGATCACCCCTACGT-3' and reverse primer 5' -CGGTCTCTACAGACAACAC-3'. PCR fragments containing the Y890F mutation are undigested by *Sna*BI (107bp), whereas WT fragments are digested (89bp) (Fig. 1E). Genotyping for the mdx point mutation was performed by PCR amplification of a 157bp fragment of the *Dmd* gene using the forward primer 5' -GCAAAGTTCTTTGAAAGGTCAA-3' and the reverse primer 5' -CACCAACTGGGAGGAAAGTT-3'. PCR fragments containing the mdx point mutation are undigested by *Hinc*II whereas WT fragments are digested (137bp) Fig. 1E.

Histology and pathophysiology—Samples of quadriceps muscle were dissected from 4–6 week old animals and processed for haematoxylin and eosin staining as described previously (43). Similarly prepared 6µm cryosections were also labelled for individual components of the dystrophin glycoprotein complex using the following antibodies: anti-αDG (VIA4-1) (1:50, 4°C, Upstate biotechnology), anti-βDG (Mandag2, 1:10, 4°C), anti-αSG (1:100, 23°C, Novocastra), anti-βSG (1:50, 23°C, Novocastra), anti-laminin-α2 (1:100, 23°C, ENZO life sciences), anti-utrophin (Rab5 rabbit polyclonal c-terminal, 1:4000, 23°C), anti-pan plectin #46 (1:200, 4°C, a gift from Gerhard Wiche, Vienna), anti-dystrophin (DYS1, 1:20 4°C, Novocastra), anti-sarcospan (PGM2, 1:50 4°C, BioServUK Ltd, UK). The PGM2 Rabbit polyclonal antibodies to murine Sspn were raised using a synthetic peptide (Sspn aa 3-16, GenBank accession number U02487, SI-Biologics Ltd, UK). Antibodies were affinity purified from rabbit serum before use.

A mouse on mouse kit was used with all primary mouse antibodies (M.O.M.TM Kit, Vector, Burlingame, CA) and the manufacturer's protocol was followed. Sections were mounted in Hydromount (National Diagnostics, Atlanta, Georgia, USA) containing 1% DABCO (Sigma-Aldrich). Fluorescence was visualised using a ZEISS AXIOSKOP 2 microscope and images were captured using QCapture software.

The number of fibres with centrally placed nuclei was determined by staining sections of quadriceps muscle with an anti-laminin-α2 antibody (as above) to delineate individual fibres with DAPI counterstain to visualise nuclei. Central nuclei were counted using cell counter in Image J 64. Analysis and statistical data was calculated in Graphpad Prism. Sections of mouse quadriceps were stained for NADH to determine oxidative fibre type as described previously (44).

Sarcolemmal integrity

Levels of serum creatine kinase were measured in duplicate using a commercial CK ELISA kit (Uscn Life Science Inc. Wuhan, P.R. China) according to the manufacturer's instructions. The plate was read at 450nm on a FLUOStar Optima plate reader (BMG-LABTECH GmbH, Ortenberg, Germany) and data expressed as U/L.

***In vivo* muscle physiology**—Mice were surgically prepared as described previously (20, 45). Isometric force measurements were made from TA muscle and maximum isometric tetanic force (P_0) was determined from the plateau of the force-frequency curve (20). After completing the final isometric contraction the muscle was allowed to rest for 5 minutes before the eccentric contraction protocol was initiated. A tetanic contraction was induced using a stimulus of 120Hz for 700ms. During the last 200ms of this contraction the muscle was stretched by 10% of L_0 at a velocity of $0.5L_0 s^{-1}$ and relaxed at $-0.5L_0 s^{-1}$. The isometric tension recorded prior to the first stretch was used as a baseline. The muscle was then subjected to 10 eccentric contractions separated by a 2 minute rest period to avoid the confounding effect of muscle fatigue. The isometric tension prior to each stretch was recorded and expressed as a percentage of the baseline tension. (20) The mouse was then euthanised and the muscle was carefully removed and weighed.

***In vitro* assays and western blotting**

Cell surface biotinylation assays—*H2kb-tsA58* mouse myoblasts (18) maintained as described previously (46), were placed on ice, washed three times in chilled PBS and incubated for 30min with 0.5 mg/ml Sulfo-NHS-SS-Biotin (Thermo Scientific) in PBS on ice. Cells were washed three times with serum free media to remove uncoupled biotin and returned to 37°C to allow endocytosis to proceed. At various time points cells were placed on ice and washed twice in chilled MesNa stripping buffer (50mM Tris-HCL pH 8.6, 100mM NaCl, 1mM EDTA), followed by 3 x 20 min washes in chilled MesNa stripping buffer with 0.2% BSA (w/v) and 100mM MesNa (Sigma) added fresh. Cells were then washed in chilled PBS containing 500mM iodoacetamide (Sigma) and left on ice for 10min, before being washed a further three times in chilled PBS before lysis in radioimmunoprecipitation buffer (6). As a control for stripping, the experiment was repeated as above, except the cells were not incubated at 37°C but were stripped immediately after biotinylation and washing with serum free media. Samples were analysed by SDS-PAGE and western blotting for phosphorylated and non-phosphorylated β -dystroglycan and transferrin receptor as control. SDS-PAGE and western blotting of muscle samples was carried out as below and described previously (6, 22, 47).

Quantification of muscle proteins—Hamstring muscle was snap frozen in liquid nitrogen and stored at -80°C prior to use. Approximately 100mg of tissue was weighed, ground to a powder under liquid nitrogen, resuspended in RIPA buffer (6) at a ratio of 1ml per 100mg of tissue and homogenised in a dounce homogeniser for 10 strokes. Samples were incubated on a roller for 30min at 4°C, before sonicating and centrifuging at 15000g for 15min. Supernatant was resuspended in Laemmli sample buffer, boiled for 10min and 30 μ l was run out on 4-15% Criterion TGX polyacrylamide gels (BioRad). Following transfer and blotting as above, chemiluminescence signals were imaged on a Chemidoc XRS+ (Biorad). Quantification was carried out in Image Lab software (Biorad) using volume measurements for each band with rolling disk background subtraction (diameter 10mm). Values were normalized against concavalin A lectin signal and represented as a ratio of the average wild type signal for each antibody. Primary Antibodies; β -DG (43Dag1 1:50, Vector Labs), pY β -DG (1709 1:1000), utrophin (Rab5 rabbit polyclonal c-terminal 1:5000), plectin (#46 1:3000, a kind gift from Gehard Wiche), dystrophin (DYS1 1:100, Novacastra) and concavalin A lectin biotin conjugate (1:2500, Vector Labs). Secondary antibodies; peroxidase conjugated anti-mouse raised in goat (1:10000 Sigma-Aldrich), peroxidase conjugated anti-rabbit raised in goat (1:20000 Sigma-Aldrich) and peroxidase conjugated extravidin (Sigma-Aldrich 1:10000).

Unless otherwise stated, statistical significance was ascertained using a 1 way ANOVA analysis with a threshold of $P < 0.05$. Tukey's multiple comparison test used for pairwise comparisons. All analyses were performed using Graphpad Prism software.

Supplementary Material

Refer to Web version on PubMed Central for supplementary material.

Acknowledgements

This work was supported by the Medical Research Council [G0701129 to S.J.W. and G.M.]. We are grateful to Lynne Williams and Mohammad Roghanian for expert technical assistance, to Steve Laval (Newcastle) for *mdx* mice and to Gerhard Wiche (Vienna) for plectin antisera.

References

1. Ervasti JM, Campbell KP. A role for the dystrophin glycoprotein complex as a transmembrane linker between laminin and actin. *J Cell Biol.* 1993; 112:809–823.
2. Ervasti JM. Costameres: the Achilles' Heel of Herculean Muscle. *J Biol Chem.* 2003; 278:13591–13594. [PubMed: 12556452]
3. Winder SJ. The complexities of dystroglycan. *Trends Biochem Sci.* 2001; 26:118–124. [PubMed: 11166570]
4. Moore C, Winder SJ. Dystroglycan versatility in cell adhesion: a tale of multiple motifs. *Cell Com Signal.* 2010; 8:3.
5. Ilsley JL, Sudol M, Winder SJ. The interaction of dystrophin with β -dystroglycan is regulated by tyrosine phosphorylation. *Cell Signal.* 2001; 13:625–632. [PubMed: 11495720]
6. James M, Nuttall A, Ilsley JL, Ottersbach K, Tinsley JN, Sudol M, Winder SJ. Adhesion-dependent tyrosine phosphorylation of β -dystroglycan regulates its interaction with utrophin. *J Cell Sci.* 2000; 113:1717–1726. [PubMed: 10769203]
7. Sotgia F, Bonuccelli G, Bedford M, Brancaccio A, Mayer U, Wilson MT, Campos-Gonzalez R, Brooks JW, Sudol M, Lisanti MP. Localization of Phospho- β -dystroglycan (pY892) to an Intracellular Vesicular Compartment in Cultured Cells and Skeletal Muscle Fibers in Vivo. *Biochem.* 2003; 42:7110–7123. [PubMed: 12795607]
8. Bonuccelli G, Sotgia F, Schubert W, Park DS, Frank PG, Woodman SE, Insabato L, Cammer M, Minetti C, Lisanti MP. Proteasome Inhibitor (MG-132) Treatment of *mdx* Mice Rescues the Expression and Membrane Localization of Dystrophin and Dystrophin-Associated Proteins. *Am J Pathol.* 2003; 163:1663–1675. [PubMed: 14507673]
9. Assereto S, Stringara S, Sotgia F, Bonuccelli G, Broccolini A, Pedemonte M, Traverso M, Biancheri R, Zara F, Bruno C, et al. Pharmacological Rescue of the Dystrophin Complex in Duchenne and Becker Skeletal Muscle Explants by Proteasomal Inhibitor Treatment. *Am J Physiol Cell Physiol.* 2006; 290:C577–582. [PubMed: 16192300]
10. Cox GA, Sunada Y, Campbell KP, Chamberlain JS. Dp71 can restore the dystrophin-associated glycoprotein complex in muscle but fails to prevent dystrophy. *Nature Genet.* 1994; 8:333–339. [PubMed: 7894482]
11. Greenberg DS, Sunada Y, Campbell KP, Yaffe D, Nudel U. Exogenous Dp71 restores the levels of dystrophin-associated proteins but does not alleviate muscle damage in *mdx* mice. *Nature Genet.* 1994; 8:340–344. [PubMed: 7894483]
12. Hoyte K, Jayasinha V, Xia B, Martin PT. Transgenic Overexpression of Dystroglycan Does Not Inhibit Muscular Dystrophy in *mdx* Mice. *Am J Pathol.* 2004; 164:711–718. [PubMed: 14742274]
13. Ervasti JM, Ohlendieck K, Kahl SD, Gaver MG, Campbell KP. Deficiency of a glycoprotein component of the dystrophin complex in dystrophic muscle. *Nature.* 1990; 345:315–319. [PubMed: 2188135]
14. Batchelor C, Winder S. Sparks, signals and shock absorbers: how dystrophin loss causes muscular dystrophy. *Trends Cell Biol.* 2006; 16:198–205. [PubMed: 16515861]
15. Nguyen T, Ellis JM, Love DR, Davies KE, Gatter KC, Dickson G, Morris GE. Localization of the DMDL gene-encoded dystrophin-related protein using a panel of nineteen monoclonal antibodies: Presence at neuromuscular junctions, in the sarcolemma of dystrophic skeletal muscle in vascular and other smooth muscles, and in proliferating brain cell lines. *J Cell Biol.* 1991; 115:1695–1700. [PubMed: 1757469]
16. Matsumura K, Ervasti JM, Ohlendieck K, et al. Association of dystrophin-related protein with dystrophin-associated protein in *mdx* mouse muscle. *Nature.* 1992; 360:588–591. [PubMed: 1461282]

17. Cluchague N, Moreau C, Rocher C, Pottier S, Leray G, Cherel Y, Le Rumeur E. beta-Dystroglycan can be revealed in microsomes from mdx mouse muscle by detergent treatment. *FEBS Letters*. 2004; 572:216–220. [PubMed: 15304351]
18. Morgan JE, Beauchamp JR, Pagel CN, Peckham M, Ataliotis P, Jat PS, Noble MD, Farmer K, Partridge TA. Myogenic Cell Lines Derived from Transgenic Mice Carrying a Thermolabile T Antigen: A Model System for the Derivation of Tissue-Specific and Mutation-Specific Cell Lines. *Dev Biol*. 1994; 162:486–498. [PubMed: 8150209]
19. Pereboev A, Ahmed N, Man Nt, Morris G. Epitopes in the interacting regions of beta-dystroglycan (PPxY motif) and dystrophin (WW domain). *Biochim Biophys Acta*. 2001; 1527:54–60. [PubMed: 11420143]
20. Sharp PS, Bye-a-Jee H, Wells DJ. Physiological Characterization of Muscle Strength With Variable Levels of Dystrophin Restoration in mdx Mice Following Local Antisense Therapy. *Mol Ther*. 2011; 19:165–171. [PubMed: 20924363]
21. Tinsley JM, Potter AC, Phelps SR, Fisher R, Trickett JI, Davies KE. Amelioration of the dystrophic phenotype of *mdx* mice using a truncated utrophin transgene. *Nature*. 1996; 384:349–353. [PubMed: 8934518]
22. Rezniczek GA, Konieczny P, Nikolic B, Reipert S, Schneller D, Abrahamsberg C, Davies KE, Winder SJ, Wiche G. Plectin 1f scaffolding at the sarcolemma of dystrophic (*mdx*) muscle fibers through multiple interactions with β -dystroglycan. *J Cell Biol*. 2007; 176:965–977. [PubMed: 17389230]
23. Konieczny P, Fuchs P, Reipert S, Kunz WS, Zeold A, Fischer I, Paulin D, Schroder R, Wiche G. Myofiber integrity depends on desmin network targeting to Z-disks and costameres via distinct plectin isoforms. *The Journal of Cell Biology*. 2008; 181:667–681. [PubMed: 18490514]
24. Goyenvalle A, Seto JT, Davies KE, Chamberlain J. Therapeutic approaches to muscular dystrophy. *Human Molecular Genetics*. 2011; 20:R69–R78. [PubMed: 21436158]
25. Pichavant C, Aartsma-Rus A, Clemens PR, Davies KE, Dickson G, Takeda Si, Wilton SD, Wolff JA, Wooddell CI, Xiao X, et al. Current Status of Pharmaceutical and Genetic Therapeutic Approaches to Treat DMD. *Mol Ther*. 2011; 19:830–840. [PubMed: 21468001]
26. Deconinck AE, Rafael JA, Skinner JA, Brown SC, Potter AC, Metzinger L, Watt DJ, Dickson JG, Tinsley JM, Davies KE. Utrophin-dystrophin-deficient mice as a model for Duchenne muscular dystrophy. *Cell*. 1997; 90:717–727. [PubMed: 9288751]
27. Grady RM, Teng H, Nicholl MC, Cunningham JC, Wilkinson RS, Sanes JR. Skeletal and cardiac myopathies in mice lacking utrophin and dystrophin: a model for Duchenne muscular dystrophy. *Cell*. 1997; 90:729–738. [PubMed: 9288752]
28. Sotgia F, Lee H, Bedford M, Petrucci TC, Sudol M, Lisanti MP. Tyrosine phosphorylation of β -dystroglycan at its WW domain binding motif, PPxY, recruits SH2 domain containing proteins. *Biochemistry*. 2001; 40:14585–14592. [PubMed: 11724572]
29. Bonuccelli G, Sotgia F, Capozza F, Gazzo E, Minetti C, Lisanti MP. Localized treatment with a novel FDA-approved proteasome inhibitor blocks the degradation of dystrophin and dystrophin-associated proteins in *mdx* mice. *Cell Cycle*. 2007; 6:1242–1248. [PubMed: 17495527]
30. Gazzo E, Assereto S, Bonetto A, Sotgia F, Scarfì S, Pistorio A, Bonuccelli G, Cilli M, Bruno C, Zara F, et al. Therapeutic Potential of Proteasome Inhibition in Duchenne and Becker Muscular Dystrophies. *Am J Pathol*. 2010; 176:1863–1877. [PubMed: 20304949]
31. Lipscomb L, Parkin CA, Juusola MI, Winder SJ. The proteasomal inhibitor MG132 prevents muscular dystrophy in zebrafish. *PLoS Currents*. 2011; 3:RRN1286. [PubMed: 22130468]
32. Karpati G, Carpenter S, Morris GE, Davies KE, Guerin C, Holland P. Localization and quantitation of the chromosome 6-encoded dystrophin-related protein in normal and pathological human muscle. *J Neuropathol Exp Neurol*. 1993; 52:119–128. [PubMed: 8440993]
33. Clerk A, Morris GE, Dubowitz V, Davies KE, Sewry CA. Dystrophin-related protein, utrophin in normal and dystrophic human fetal skeletal muscle. *Histochem J*. 1993; 25:554–561. [PubMed: 8407365]
34. Tinsley JM, Fairclough RJ, Storer R, Wilkes FJ, Potter AC, Squire SE, Powell DS, Cozzoli A, Capogrosso RF, Lambert A, et al. Daily Treatment with SMTC1100, a Novel Small Molecule

- Utrophin Upregulator, Dramatically Reduces the Dystrophic Symptoms in the mdx Mouse. *PLoS One*. 2011; 6:e19189. [PubMed: 21573153]
35. Smith FJD, Eady RAJ, Leigh IM, McMillan JR, Rugg EL, Kellsell DP, Bryant SP, Spurr NK, Geddes JF, Kirtschig G, et al. Plectin deficiency results in muscular dystrophy with epidermolysis bullosa. *Nature Genet*. 1996; 13:450–457. [PubMed: 8696340]
 36. Andrä K, Lassmann H, Bittner R, Shorny S, Fässler R, Propst F, Wiche G. Targeted inactivation of plectin reveals essential function in maintaining the integrity of skin, muscle, and heart cytoarchitecture. *Genes & Dev*. 1997; 11:3143–3156. [PubMed: 9389647]
 37. Pulkkinen L, Smith FJD, Shimizu H, Murata S, Yaoita H, Hachisuka H, Nishikawa T, McLean WHI, Uitto J. Homozygous Deletion Mutations in the Plectin Gene (PLEC1) in Patients with Epidermolysis Bullosa Simplex Associated with Late-Onset Muscular Dystrophy. *Human Molecular Genetics*. 1996; 5:1539–1546. [PubMed: 8894687]
 38. Schröder R, Mundegar R, Treusch M, Schlegel U, Blümcke I, Owaribe K, Magin T. Altered distribution of plectin/HD1 in dystrophinopathies. *Eur J Cell Biol*. 1997; 74:165–171. [PubMed: 9352221]
 39. Gundesli H, Talim B, Korkusuz P, Balci-Hayta B, Cirak S, Akarsu NA, Topaloglu H, Dincer P. Mutation in Exon 1f of PLEC, Leading to Disruption of Plectin Isoform 1f, Causes Autosomal-Recessive Limb-Girdle Muscular Dystrophy. *Am J Hum Genet*. 2010; 87:834–841. [PubMed: 21109228]
 40. Hu H, Columbus J, Zhang Y, Wu D, Lian L, Yang S, Goodwin J, Luczak C, Carter M, Chen L, et al. A map of WW domain family interactions. *PROTEOMICS*. 2004; 4:643–655. [PubMed: 14997488]
 41. Otte L, Wiedemann U, Schlegel B, Pires JR, Beyermann M, Schmieder P, Krause G, Volkmer-Engert R, Schneider-Mergener J, Oschkinat H. WW domain sequence activity relationships identified using ligand recognition propensities of 42 WW domains. *Protein Science*. 2003; 12:491–500. [PubMed: 12592019]
 42. McArthur T, Ohtoshi A. A Brain-Specific Homeobox Gene, *Bsx*, Is Essential for Proper Postnatal Growth and Nursing. *Mol Cell Biol*. 2007; 27:5120–5127. [PubMed: 17485440]
 43. Miller G, Peter A, Espinoza E, Heighway J, Crosbie R. Over-expression of *Microspan*, a novel component of the sarcoplasmic reticulum, causes severe muscle pathology with triad abnormalities. *J Muscle Res Cell Motil*. 2006; 27:545. [PubMed: 16823602]
 44. Judge LM, Arnett ALH, Banks GB, Chamberlain JS. Expression of the dystrophin isoform Dp116 preserves functional muscle mass and extends lifespan without preventing dystrophy in severely dystrophic mice. *Human Molecular Genetics*. 2011; 20:4978–4990. [PubMed: 21949353]
 45. Foster H, Sharp PS, Athanasopoulos T, Trollet C, Graham IR, Foster K, Wells DJ, Dickson G. Codon and mRNA Sequence Optimization of Microdystrophin Transgenes Improves Expression and Physiological Outcome in Dystrophic mdx Mice Following AAV2/8 Gene Transfer. *Mol Ther*. 2008; 16:1825–1832. [PubMed: 18766174]
 46. Thompson O, Kleino I, Crimaldi L, Gimona M, Saksela K, Winder SJ. Dystroglycan, *Tks5* and *Src* mediated assembly of podosomes in myoblasts. *PLoS One*. 2008; 3:e3638. [PubMed: 18982058]
 47. Thompson O, Moore CJ, Hussain S-A, Kleino I, Peckham M, Hohenester E, Ayscough KR, Saksela K, Winder SJ. Modulation of cell spreading and cell-substrate adhesion dynamics by dystroglycan. *J Cell Sci*. 2010; 123:118–127. [PubMed: 20016072]

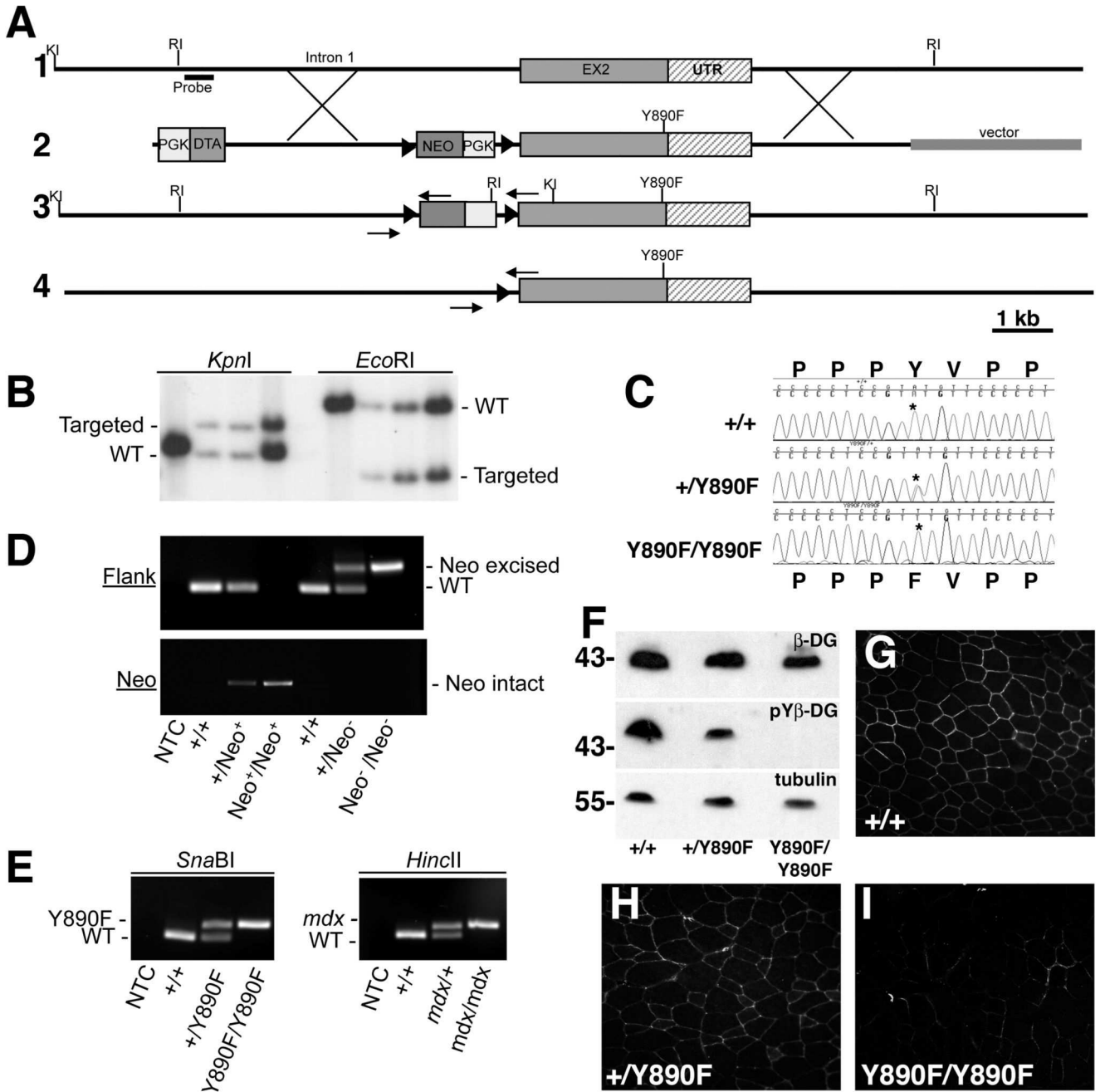


Figure 1. Generation of a *Dag1*^{Y890F} targeting construct.

A) Schematic representation of the genomic locus (1), targeting construct (2), targeted locus both with (4) and without (3) cre recombined excision of the neomycin resistance cassette are shown. Restriction sites for Southern blotting are shown KI= *KpnI* and EI = *EcoRI*. Flank and Neo PCR primers used to determine whether the neomycin resistance cassette (PGK Neo) has been excised are represented by arrows. LoxP sites flanking PGK Neo are depicted by arrowheads. The location of the probe used for Southern blotting is indicated. Scalebar = 1 kb. B) A representative Southern blot of restriction digested genomic DNA

from four different ES cell clones probed with the probe indicated in A is shown. Whether the band corresponds to a wild-type allele or a targeted allele is indicated. C) Chromatograms of sequences from progeny with the genotypes indicated on the left are shown, the A to T point mutation corresponding to Y890F is indicated with an asterisk. D) 2% agarose gel electrophoresis of PCR products from the Neo and Flank PCRs used to determine the presence or absence of the neomycin resistance cassette, the genotype of the DNA used as a template is shown on the bottom: +=wild-type allele, neo⁻=an allele with the neomycin cassette excised; neo⁺= an allele with the neomycin cassette intact, NTC= the no template control. E) 3.5% agarose gel electrophoresis of *Sna*BI and *Hinc*II digested PCR products used to genotype progeny for the Y890F and *mdx* point mutations respectively, genotypes of the samples are shown beneath. F, western blotting of quadriceps femoris samples from wildtype (+/+), heterozygote (+/Y890F) and homozygote (Y890F/Y890F) mice using antibodies against non-phosphorylated β -dystroglycan (β -DG), tyrosine phosphorylated β -DG (pY β -DG) and tubulin as a loading control. Representative immunofluorescence localisation of tyrosine phosphorylated β -DG in sections of quadriceps femoris from wildtype (+/+; G), heterozygote (+/Y890F; H) and homozygote (Y890F/Y890F; I) mice.

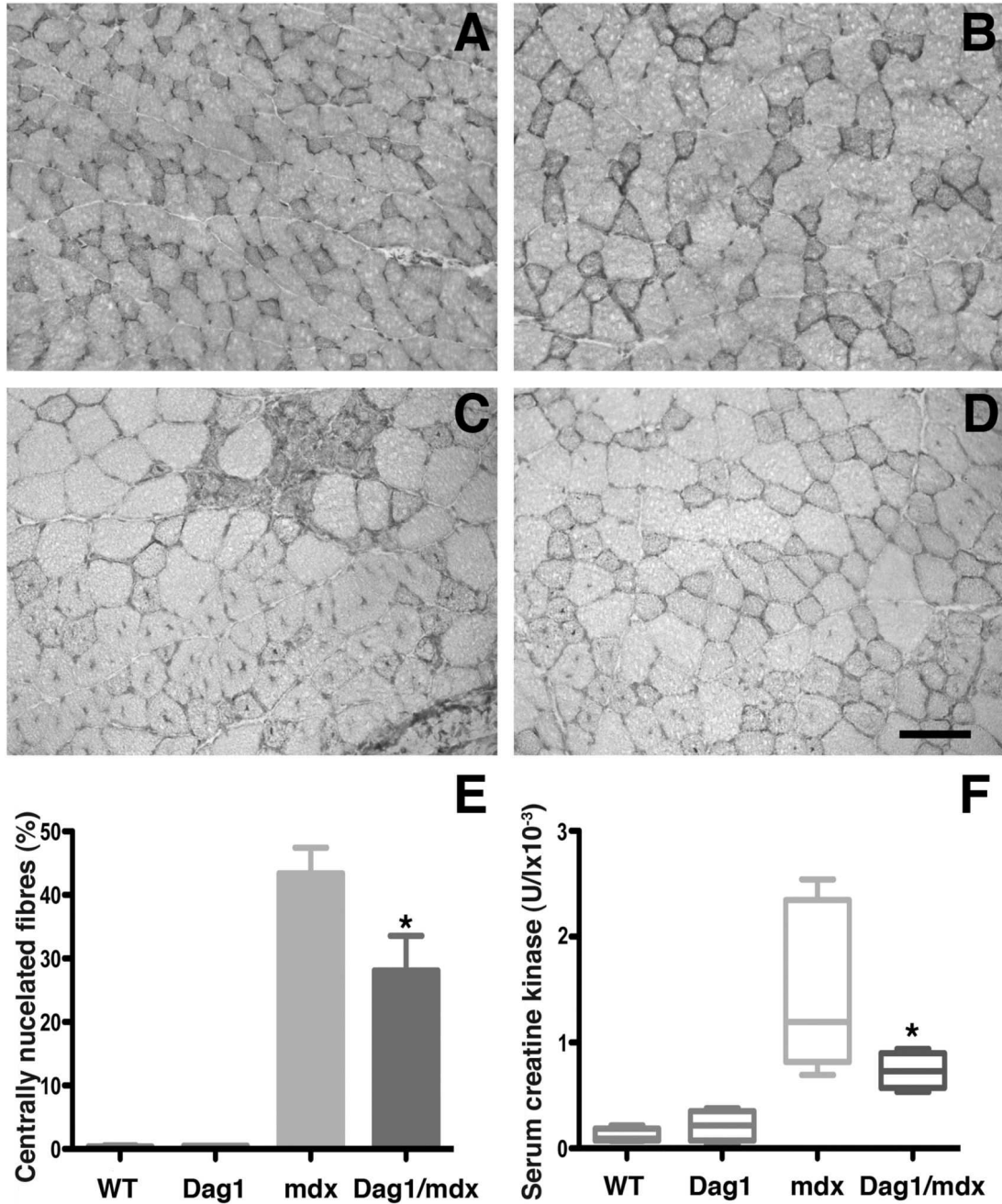


Figure 2. Pathophysiological analysis of *Dag1^{Y890F/Y890F}* and *Dag1^{Y890F/Y890F}/mdx* muscle. Haematoxylin and eosin staining of wildtype quadriceps muscle (A) is similar to *Dag1^{Y890F/Y890F}* (B) whereas when crossed to *mdx* there was improved pathology in *Dag1^{Y890F/Y890F}/mdx* (D) compared to *mdx* alone (C), with larger more even fibre size and a reduction in centrally nucleated fibres (CNF). Scale bar = 50μm. Central nucleation was quantified by counting more than 100 fibres per section from 3 different animals of the indicated genotype (E). Whilst *Dag1^{Y890F/Y890F}* had a very low number of CNF and was no different from wildtype, compared to *mdx*, *Dag1^{Y890F/Y890F}/mdx* showed a significant 30%

reduction in CNF. Mean \pm sem $p=0.043$. Serum creatine kinase (CK) levels were similarly unaffected in *Dag1*^{Y890F/Y890F} mice (n=4), whereas the introduction of *Dag1*^{Y890F/Y890F} into *mdx* (n=4) caused a dramatic and significant 50% reduction in CK levels compared to *mdx* alone (n=7; F).

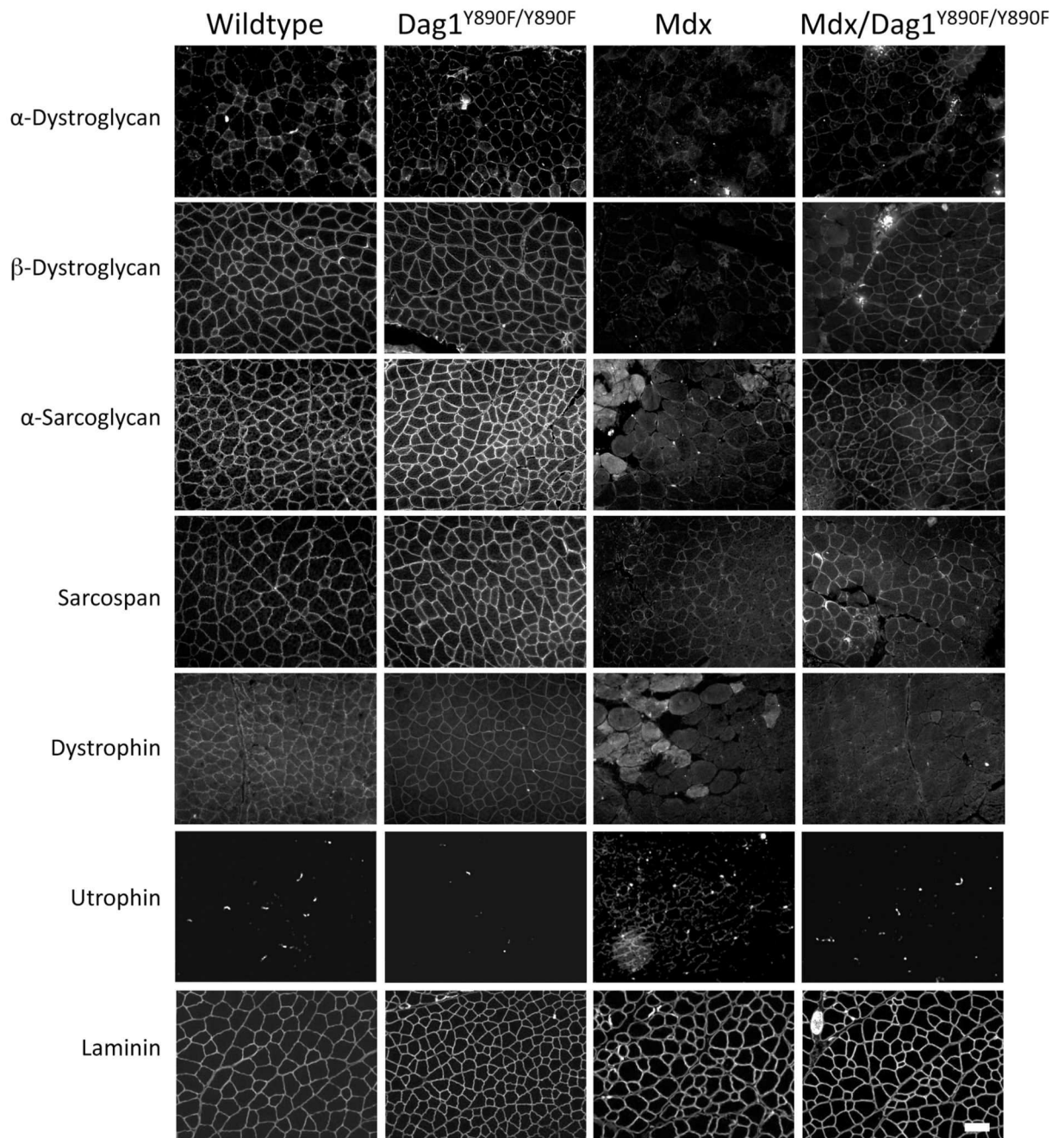


Figure 3. Restoration of DGC components in *Dag1*^{Y890F/Y890F}/*mdx* muscle.

Immunofluorescence localisation to the sarcolemma of the DGC components: α- and β-dystroglycan; α-sarcoglycan; sarcospan; dystrophin and utrophin, was unaltered in *Dag1*^{Y890F/Y890F} mice. As expected all DGC components were significantly reduced from the sarcolemma of *mdx* muscle, where laminin localisation was unaltered and utrophin showed an increased extra-synaptic localisation. In *Dag1*^{Y890F/Y890F}/*mdx* mice however, there was a clear restoration of all DGC components examined, even in the absence of dystrophin, but with a concomitant loss of utrophin staining from the sarcolemma. Some

mdx muscle fibres show internal fluorescence, which is likely to be non-specific uptake of secondary antibody by necrotic fibres. Scale bar = 50µm.

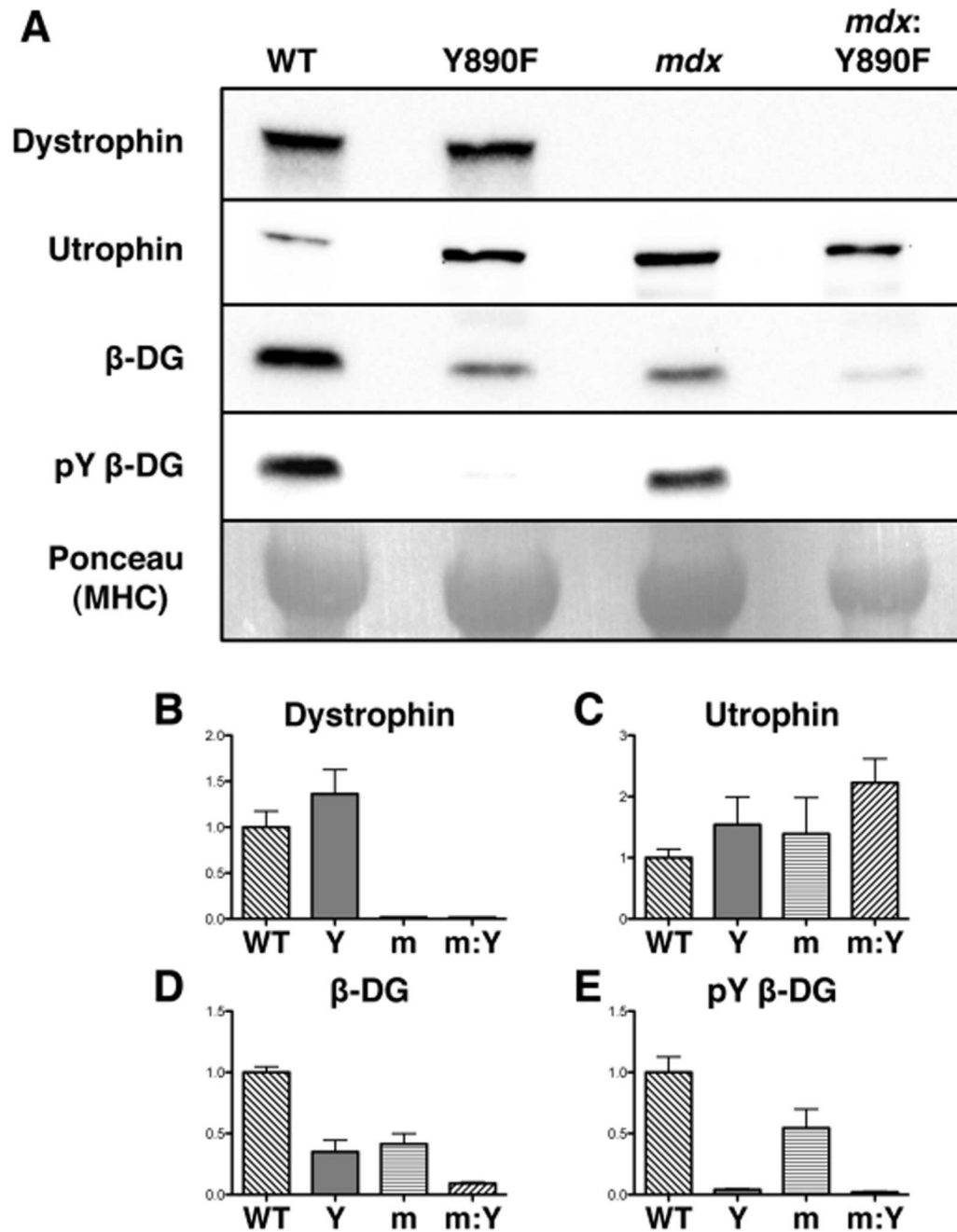


Figure 4. Western blot analysis of dystrophin, utrophin and dystroglycan.

In keeping with the genetic background of the respective animal models, dystrophin was not detectable in western blots of muscle from *mdx* (m) or *Dag1*^{Y890F/Y890F}/*mdx* Y/m mice (A,B) and pY β -dystroglycan was not detectable in muscle from *Dag1*^{Y890F/Y890F} (Y) or *Dag1*^{Y890F/Y890F}/*mdx* mice (A,E). Compared to wildtype (WT), un-phosphorylated β -dystroglycan was significantly reduced in all mice (D), but despite an upward trend in utrophin levels from WT to Y to m to Y/m, the differences were not significant (C). Data are mean \pm SEM n=4.

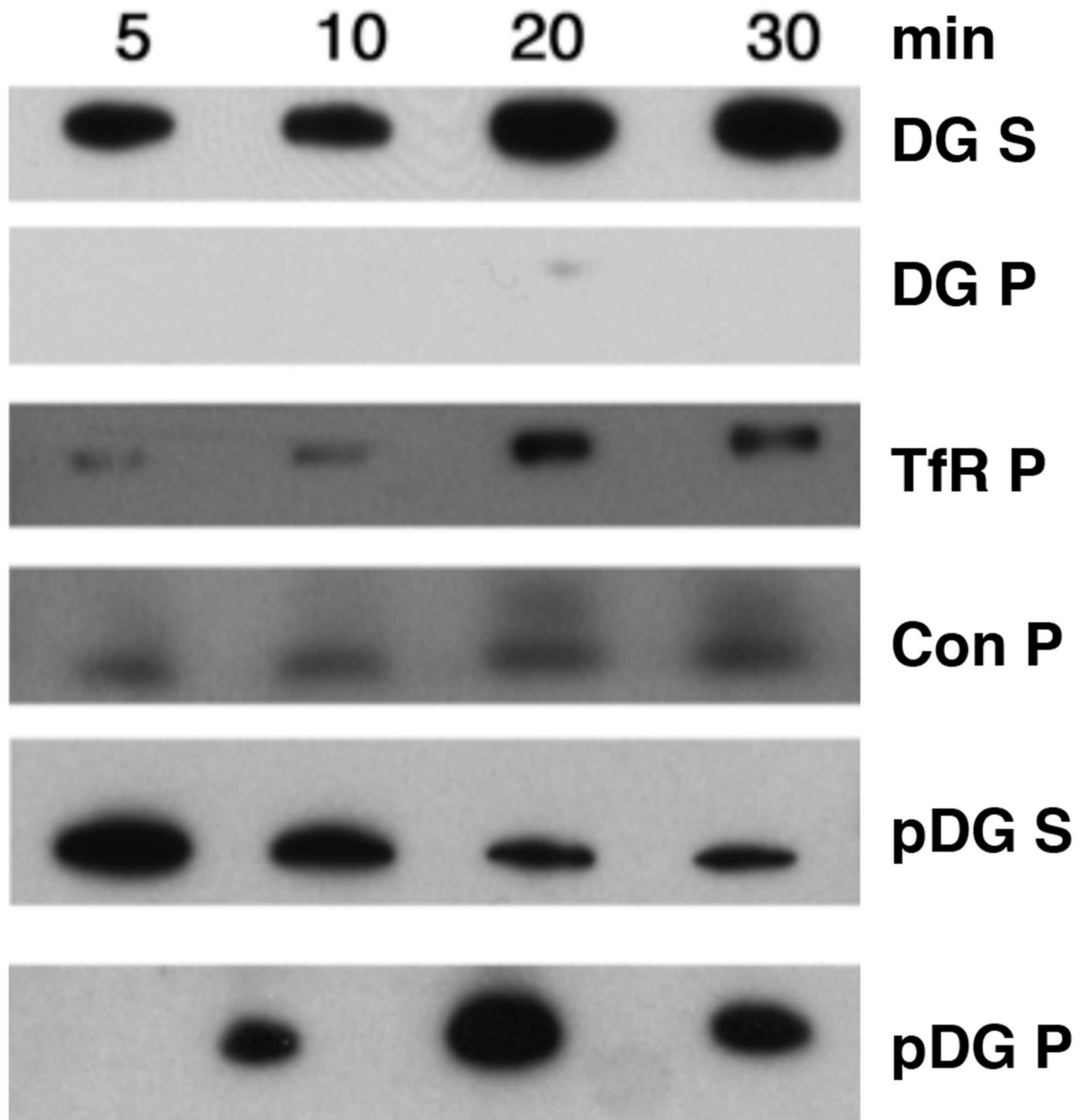


Figure 5. Internalisation of pY890 β -dystroglycan in myoblasts.

Cell surface biotinylation followed by recovery of endocytosed biotinylated proteins (A) revealed that only tyrosine phosphorylated β -dystroglycan (pDG) was internalised and recovered in the pellet fraction (pDG P) with a clear reduction over time of the surface supernatant fraction (pDG S). Unphosphorylated β -dystroglycan (DG) remained on the cell surface (DG S) with no unphosphorylated β -dystroglycan being internalised (DG P). Control western blots for transferrin receptor (TfR P) demonstrate the time course of clathrin

mediated endocytosis in these cells, and blotting of an unknown biotinylated protein (Con P) acts as a loading control.

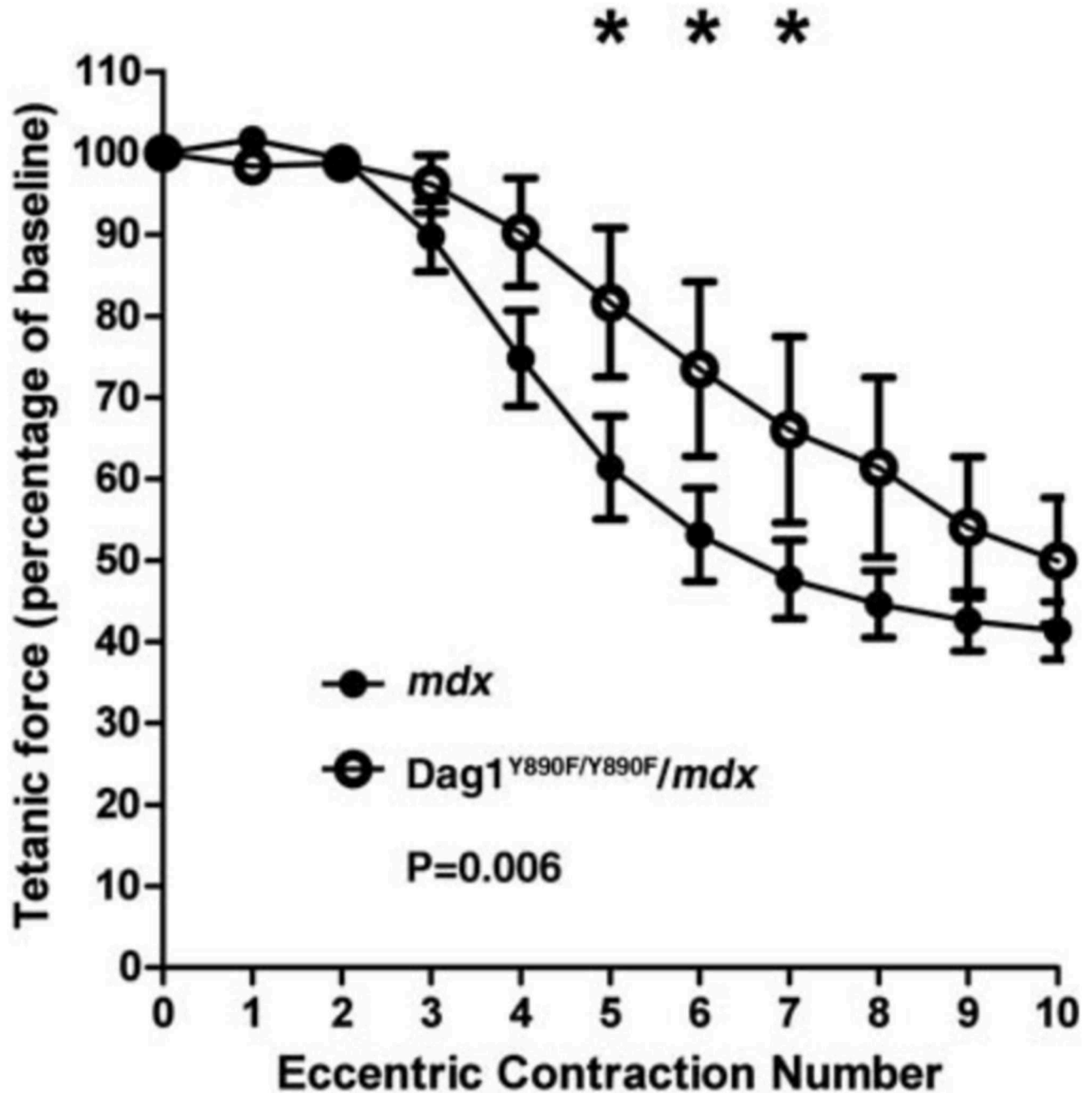


Figure 6. Resistance to contraction-induced injury in *mdx* and *Dag1^{Y890F/Y890F}/mdx* mice. The TA muscle from anaesthetised *Dag1^{Y890F/Y890F}/mdx* (n=4) and *mdx* mice (n=5) underwent a protocol of 10 eccentric contractions *in situ*. Each stretch induced a 10% increase in muscle length during a tetanic contraction. Tetanic force is expressed as a percentage of baseline isometric force produced prior to the first stretch. The drop in tetanic force was significantly reduced in *Dag1^{Y890F/Y890F}/mdx* mice compared to age-matched *mdx* controls (P=0.006). *Dag1^{Y890F/Y890F}/mdx* mice were significantly stronger than *mdx* mice at contractions 5, 6 and 7 (P=0.025, 0.025 and 0.040 respectively; Two-way Repeated

Measures ANOVA with Tukey' s Post-hoc test). TA:*tibialis anterior*. Error bars represent SEM.

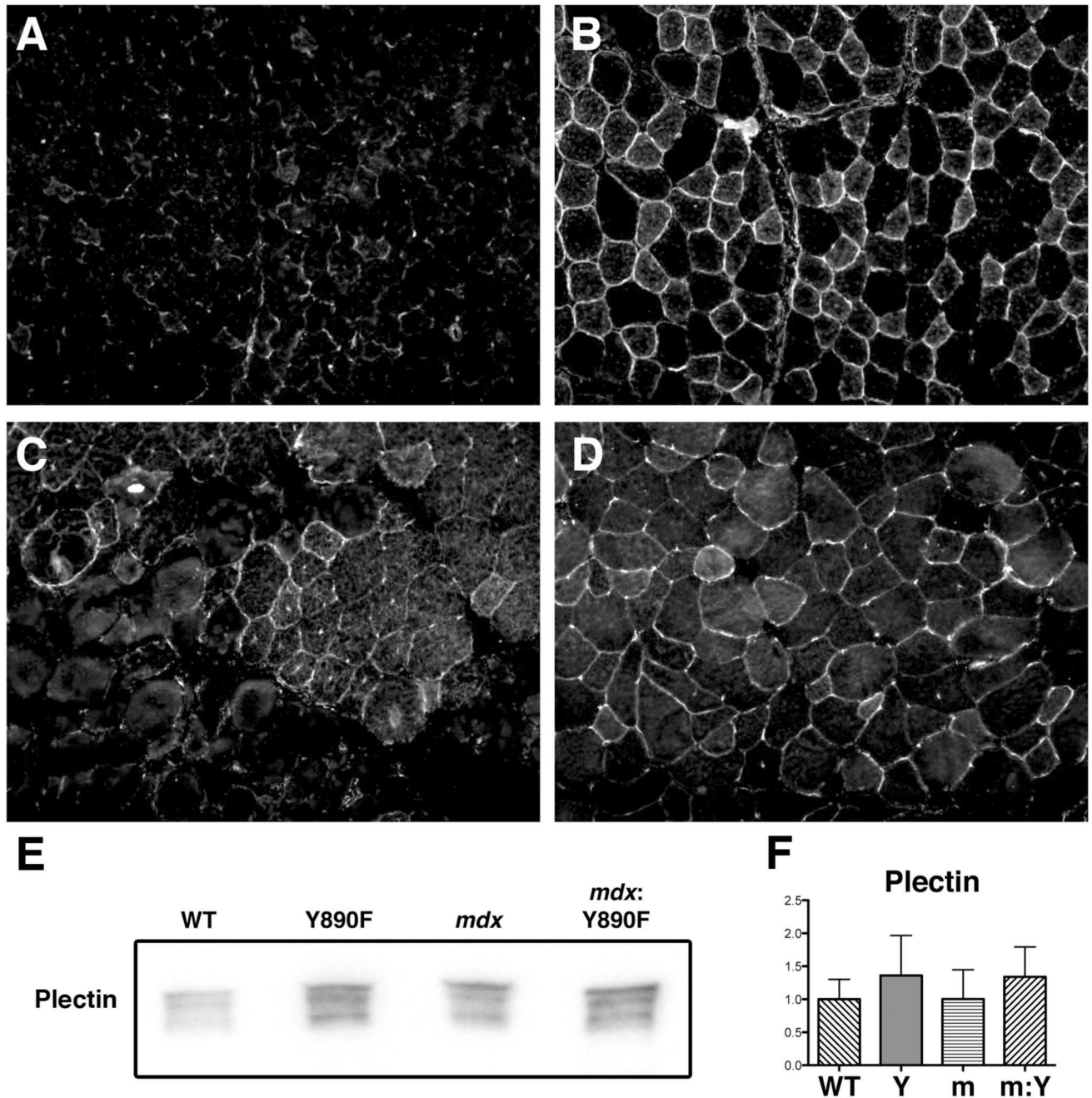


Figure 7. Plectin staining is increased at the sarcolemma of *Dag1^{Y890F/Y890F}/mdx* mice. Immunofluorescence localisation of plectin (A-D) revealed an expected increase in sarcolemmal staining in *mdx* mice, most often associated with regenerating fibres where plectin staining also localises around the central nuclei (C). However, there was also a significant localisation of plectin to the sarcolemma in *Dag1^{Y890F/Y890F}* mice (B) which was maintained at a similar level in *Dag1^{Y890F/Y890F}/mdx* mice (D). Quantification of plectin levels by western blotting in wildtype (WT), *Dag1^{Y890F/Y890F}* (Y), *mdx* (m) or *Dag1^{Y890F/Y890F}/mdx* (Y/m) mice (E,F) revealed a slight increase in plectin levels in

Dag1^{Y890F/Y890F} mice in keeping with the immunohistochemistry (B), however this increase was not significant (mean \pm SEM, n=4). Scale bar = 50 μ m.